Materials Horizons

ROYAL SOCIETY OF CHEMISTRY

REVIEW

View Article Online
View Journal | View Issue

Cite this: *Mater. Horiz.*, 2022, **9**, 112

Applications of triarylborane materials in cell imaging and sensing of bio-relevant molecules such as DNA, RNA, and proteins†

Sarina M. Berger and Todd B. Marder *

Received 27th April 2021,
Accepted 24th June 2021

DOI: 10.1039/d1mh00696g

rsc.li/materials-horizons

Triarylboranes have been known for more than 100 years and have found potential applications in various fields such as anion sensors and optoelectronics, for example in organic light emitting diodes (OLEDs), field effect transistors (OFETs), and organic photovoltaic devices. However, biological applications, such as bioimaging agents and biomolecule sensors have evolved much more recently. This review summarises progress in this relatively young field and highlights the potential of triarylboranes in biological applications.

1. Introduction

For more than 100 years, many different types of organoboron compounds have been synthesised and their potential for applications in various fields[1–3] such as anion sensors,[4–8] light emitting layers in organic light-emitting devices (OLEDs)[9,10] and electron conducting layers in organic solar cells has been clearly demonstrated.[11–13] Some types of organoboron compounds, especially boronic acids, have also been investigated for biological applications such as bioimaging agents,[14–32] or anti-cancer drugs.[33,34] However, for applications as anion sensors and bioimaging and sensing agents, organoboron compounds must be air- and moisture-stable. Therefore, the empty boron p-orbital in 3-coordinate boron compounds, which makes them good Lewis acids and susceptible to B–C bond hydrolysis, has to be stabilised. In addition, these compounds should be highly luminescent so that their localisation in tissues or in specific cell organelles can be visualised by, *e.g.*,

Institut für Anorganische Chemie and Institute for Sustainable Chemistry & Catalysis with Boron, Julius-Maximilians-Universität Würzburg, Am Hubland, 97074 Würzburg, Germany. E-mail: todd.marder@uni-wuerzburg.de

† Dedicated to Seth R. Marder on the occasion of his 60th birthday.

Sarina M. Berger

Sarina M. Berger studied chemistry at the Julius-Maximilians-University of Würzburg and completed her Bachelor's thesis in Prof. Dr Frank Würthner's group at the Institute of Organic Chemistry in 2016. She then joined Prof. Dr Todd B. Marder's group at the Institute of Inorganic Chemistry where she completed her Master's thesis in 2018, and is currently carrying out her PhD research on the synthesis and opto-electronical properties of selectively charged triarylborane chromophores.

Todd B. Marder

Todd Marder obtained his BSc from M. I. T. and PhD from UCLA. He was a postdoc in Bristol (UK), and a Visiting Scientist at DuPont before joining the faculty at the University of Waterloo (Canada). He moved to the Durham University (UK) in 1997 and to the University of Würzburg (Germany) in 2012, both times as Chair of Inorganic Chemistry. Honors: Rutherford Memorial Medal for Chemistry (Canada), RSC Awards in Main Group and Organometallic Chemistry, JSPS Fellowship, Humboldt Research Award, Royal Society Wolfson Research Merit Award, member: Bavarian Academy of Sciences, fellow: RSC, AAAS, EurASc, Honorary Professorships, etc. in UK, France, Hong Kong, China, Japan, India and Australia.

confocal fluorescence microscopy for imaging purposes. For sensing, upon interaction with the molecule to be detected, a change in emission is required. This can include a quenching of the emission, known as a 'turn-off' sensor, or a significant change in the emission wavelength. If compounds which are not inherently emissive are used, they should respond to a biological trigger resulting in a luminescence signal, which is known as a 'turn-on' sensor. In addition, it is useful to employ compounds which have large two-photon absorption cross-sections (σ_2) which allow the use of lower energy near infrared (NIR) excitation. As biological systems are relatively transparent in the NIR region of the spectrum, such systems provide deeper tissue penetration and lower background emission from biomolecules. This approach also provides a higher degree of 3D spatial resolution as the simultaneous absorption of two lower energy photons is proportional to the square of the excitation light intensity, which in turn is proportional to the square of the distance from the focal plane.

Several strategies have been developed to stabilise boron compounds for applications in aqueous media. One possibility is to bind a Lewis base to the empty p-orbital which results in 4-coordinate boron compounds, for example, boranophosphates (**1**, Scheme 1), 4-bora-3α,4α-diaza-*s*-indacene cored compounds (BODIPYs, **2**) or amine-boranes (**3**). Boranophosphates have been synthesised as mimics of nucleotides, DNA, and RNA and their biological activity has been investigated as summarised by Shaw *et al.*[33] Furthermore, some derivatives of amine-boranes have shown potential application as anticancer agents.[34] In addition to the possible applications of BODIPYs in OLEDs,[10,35–37] their biological applicability has been investigated more recently, especially as compounds for positron emission tomography (PET),[38] as fluorescence indicators[39] and, more generally, in medical diagnostics and treatment.[40,41]

Another set of air- and moisture-stable boron compounds are polyhedral clusters (**4**). For more than 30 years, different clusters have been attached to various natural compounds such as nucleosides, peptides, antibodies, *etc.*, for applications of the resulting compounds in boron-neutron capture therapy (BNCT) for cancer treatment.[42–45]

However, for 3-coordinate organoboron compounds, the empty p-orbital of the boron centre can be stabilised, *e.g.*, by using π-electron-donating atoms such as oxygen in boronic acids and esters (**5**). One of the most prominent examples of boronic acids in biological applications is Bortezomib (Scheme 1), sold as Valcade® since 2003 for the treatment of different types of cancer.[46] Other compounds containing a boronic ester motif are of current interest as they react with hydrogen peroxide (H_2O_2) to yield the corresponding alcohol (Scheme 1)[47–50] which might be useful for the treatment of diabetes, neurodegenerative disorders, or cancer.[51]

Triarylboranes (**6**) can be stabilised by sterically demanding aryl groups such as 2,6-xylyl, mesityl or tri-iso-propylphenyl (Tip),[5,14,17,18,21,22,24,26,28,30,52–55] which shield the empty p-orbital from nucleophilic attack by, *e.g.*, water. This general approach was used for all triarylboranes presented in the following sections. Attaching 2,6-xylyl, pyrenyl, 9-anthracenyl, or similar sterically-demanding substituents can yield compounds which are not only air- and moisture-stable but also water-soluble by incorporation of water-insoluble triarylboranes into water-soluble polymers or attachment of hydrophilic moieties such as biomolecules or cationic moieties. Selected examples of such triarylboranes which were investigated in cells were mentioned in reviews,[56–58] but the subject has not yet been summarised. As this is a very young and promising field which may lead to applications of triarylboranes in bioimaging (or maybe even cancer treatment), we summarise and discuss results that have been obtained to date and provide a perspective on directions this field might take.

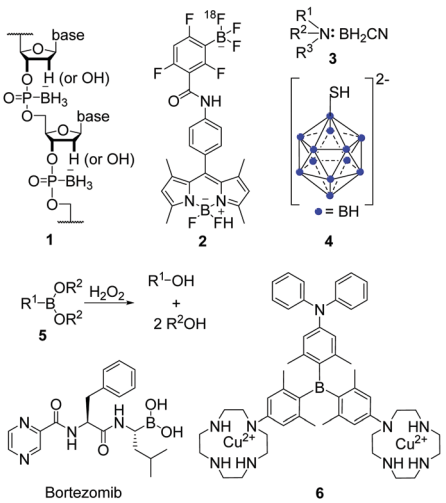

Scheme 1 Exemplary structures of boranophosphates (**1**),[33] BODIPYs (**2**),[38] amine-boranes (**3**),[34] boron clusters (**4**),[43] boronic acids and esters (**5**) and their reaction with hydrogen peroxide (H_2O_2),[46] and triarylboranes (**6**)[1] investigated for their potential in biological applications.

2. Triarylborane-loaded nanogels

Triarylboranes that are not water-soluble can be incorporated into polymeric structures by either covalent bonding between the triarylborane and the polymer (**7**, Scheme 2) or by hydrophilic and hydrophobic interactions between the host (polymer) and the guest (triarylborane; **8**, **9**, **10**), which leads to water-soluble and cell permeable structures. Yang and co-workers, in cooperation with Hu, S. Li, Y. Li, Zhu, Zhang, and Shen, showed that this approach can lead to cell permeable polymers which stain the cytoplasm and give a fluorometric response to biothiols (**8**),[15] to changes of temperature (**7**)[16] or pH (**10-OH**),[20] and to H_2O_2 (**10**),[20] depending on the structure of the triarylborane. Furthermore, they showed that such nanogels are non-toxic to mouse fibroblast (NIH/3T3) cells up to concentrations of 0.4 μg mL^{-1}.

Triarylborane **8** bears a maleimide functionality which reacts selectively with biothiols, namely cysteine, homocysteine and glutathione, resulting in a turn-on fluorescence response

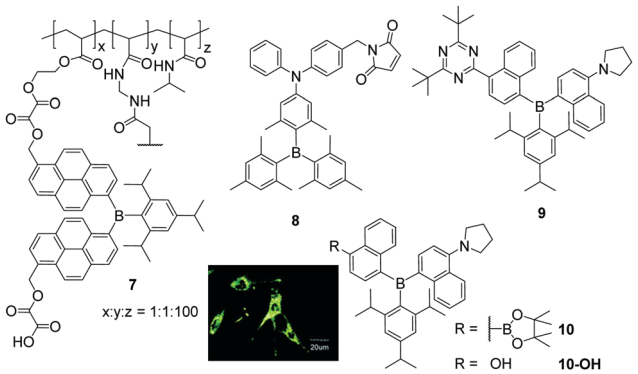

Scheme 2 Molecular structures of compounds **7**,[16] **8**,[15] **9**,[19] and **10**.[20] Coloured picture depicts localisation of **NG-10** in NIH/3T3 cells. Picture is reproduced from ref. 20 with permission from the Centre National de la Recherche Scientifique (CNRS) and The Royal Society of Chemistry.

within 10, 30 or 120 min, respectively.[15] To monitor temperature changes inside NIH/3T3 cells, compound **7** consists of a triarylborane motif covalently bound to a polymeric backbone which changes its structure from coiled to globular upon increasing temperature.[16] To obtain a stronger fluorometric response, **7** was mixed with the commercially available chromophore Nile red, which leads to a nanogel with a reversible colour change in the stained cells from red at 25 °C to greenish at 37 °C. Donor–π–acceptor compound **9** was incorporated into a polymeric structure to provide a fluorometric response to changes of polarity (solvatochromism) and viscosity inside cells.[19] Although the triarylborane itself was reported to show aggregation induced emission (AIE), inside the cell no differences in fluorescence were observed. However, from the staining pattern obtained, the authors concluded that, inside NIH/3T3 cells, the water-insoluble triarylborane **9** leaves the nanogel and aggregates in the cytoplasm, which leads to bright dots. Furthermore, they assumed that **9** enters the cell nucleus as single molecules. Similar behaviour was reported for **NG-10**, a nanogel loaded with compound **10**, which gives a fluorometric response to H_2O_2 due to cleavage of its boronic ester moiety (Scheme 2),[20] and subsequent formation of a C–O bond yielding **NG-10-OH**, which changes the emission colour from yellow to blue. In turn, **NG-10-OH** was shown to respond to cellular pH.

3. Neutral triarylboranes

Another way to obtain triarylboranes which are water-soluble at concentrations required for biological applications is by attaching hydrophilic groups such as secondary amines or amides. The groups of Thilagar and Yang showed that specifically designed triarylboranes can stain different parts of cells selectively depending on the nature of their periphery. Thus, Thilagar and co-workers prepared a thiophenol sensor (**11a** and **11b**) by attaching a 2,4-dinitrobenzenesulfonyl (DNBS) moiety to a triarylborane resulting in a turn-on fluorescence sensor for

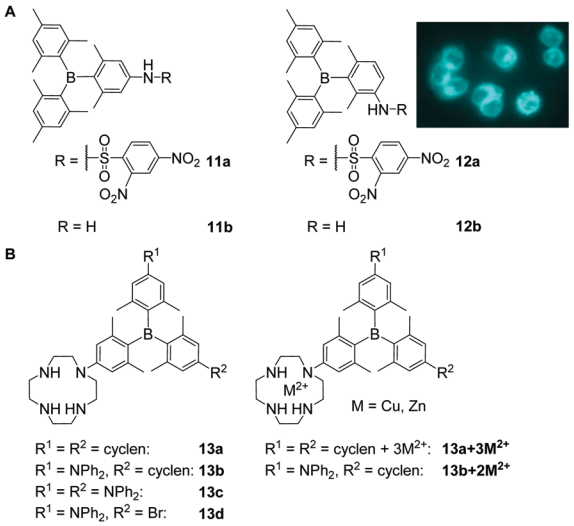

Scheme 3 (A) Structures of compounds **11** and **12** reported by Thilagar and co-workers. The coloured picture shows the turn-on fluorescence sensing of thiophenol in HeLa cells. The picture is reprinted with permission from ref. 23. © 2018 American Chemical Society.[23] (B) Cyclen-substituted triarylboranes **13a–d**, **13a + 3M²⁺**, **13b + 2M²⁺** (M = Zn, Cu) reported by Yang and co-workers.[18,21,29,32]

thiophenol in human cervical cancer (HeLa) cells (Scheme 3A).[23] Compounds **11a** and **12a** were reported to have low cytotoxicity.

Yang, Zhu, Zhang, Liu, Leng, Xu, Fu, S. Li, Y. Li and co-workers reported a series of cyclen-substituted triarylboranes (**13a–d**, **13a + 3M²⁺**, **13b + 2M²⁺**) that sense H_2S (**13b + 2Cu²⁺**),[18] RNA (**13b + 2Zn²⁺**,[29] **13b**)[21] or monoamine oxidase (MAO) at the surface of mitochondria (**13b**)[32] in, *e.g.*, human breast cancer (MCF-7) and human liver carcinoma (HepG2) cells. Compound **13b** was reported to enter NIH/3T3 cells within 5 min and to stain the cytoplasm and nucleoli, the latter most likely due to RNA binding which was indicated by co-localisation experiments with SYTO™ RNAselect™.[21] Low cytotoxicity was reported for the water-soluble compound **13b**.[32] With an incubation time of over 1 h, **13a** and **13c** give rise to weak fluorescence in NIH/3T3 cells, but the staining pattern was not investigated further.[18] The same compounds **13a–13d** were reported by Leng, Liu and co-workers for the selective sensing of monoamine oxidases (MAOs).[32] In this more recent study, the low cytotoxicity of **13b** as well as its ability to enter cells was confirmed, whereas the staining pattern reported in NIH/3T3 cells was not. Complexation of **13b** with Cu^{2+} gives **13b + 2Cu²⁺**, which enters NIH/3T3 cells, is not cytotoxic, and stains the cytoplasm and the mitochondria as indicated by co-localisation experiments with MitoTracker™ DeepRed FM (MTDF).[18] It was proposed that the latter results most likely from the presence of H_2S in the mitochondria. Using Zn^{2+} instead of Cu^{2+} gives **13b + 2Zn²⁺** which enters NIH/3T3 cells within 30 min and stains the nucleolus, the cell membrane, lysosomes, mitochondria, and the endoplasmic reticulum,[29] as indicated by extensive co-localisation studies. Localisation in the nucleoli, cell membrane, and endoplasmic reticulum of NIH/3T3 cells was attributed to the ability of **13b + 2Zn²⁺** to bind to RNA in the cell

nucleus and to localise in hydrophobic regions of the cells. A similar staining pattern was reported for the compound in HeLa cells whereas slightly different staining patterns were observed in HepG2 cells, which Yang and co-workers attributed to higher viscosity and therefore slower distribution of **13b** + **2Zn**$^{2+}$ in the latter cell line. The compound is not cytotoxic to any of the cell lines tested.

With a series of piperazine-modified triarylboranes (**14**, **15**, **16** and **17a–d**), Yang, Zhu, Zhang, Liu and co-workers showed that biomolecules such as cyclic pentapeptides, namely cRGD, can be attached to the triarylborane core (**16**, **17a–d**). These compounds are able to enter the cell nucleus (**15**)[22] and to differentiate between healthy cells and cancer cells by binding to integrin $\alpha_V\beta_3$ (**16**)[27] or by reacting with γ-glutamyl-transpeptidase (GGT; **17b**).[28] In aqueous solution, **14** and **15** were found to bind RNA preferentially over DNA.[22] Without reporting the cytotoxicity of these compounds, NIH/3T3 cells were incubated with **14** and **15** and staining of the cytoplasm and the nucleoli was observed, the latter indicated by co-localisation experiments with SYTO™ RNAselect™. For **15**, staining of the nuclear matrix, the nuclear membrane and the nuclear pore was indicated by confocal microscopy. From fluorescence lifetime microscopy (FLIM) measurements, Yang, Zhu, Zhang and co-workers concluded that the polarity in the centre of the nucleolus is lower than at its border. However, in another report by Zhang, Liu, Yang and co-workers, no specific binding to the nucleoli, the nuclear membrane or matrix was mentioned for **15**.[27]

Triarylborane **16** (Scheme 4) was designed to distinguish tumour cells from healthy cells by not staining the latter ones as they do not overexpress integrin $\alpha_V\beta_3$.[27] This was demonstrated by selective staining of human umbilical vein endothelial (HUVEC-1) and human primary glioblastoma (U87MG) cells over NIH/3T3 cells and pre-incubation studies with free cRGD. In contrast, all three cell lines were stained by the unmodified triarylborane **15**. As no cytotoxicity of compound **16** was observed, *in vivo* tests to image a tumour selectively in mice showed that the triarylborane stains the tumour within 60 min and exhibits bright fluorescence for another 30 min.

To obtain a fluorescent probe for the detection of GGT, **15** was modified with a peptide yielding **17b** (Scheme 4), which can be hydrolysed by GGT in two steps leading to **17c** and **15**, and enhancement of the fluorescence was observed.[28] Compound **17b** does not enter HUVEC-1 or NIH/3T3 cells but does enter ovarian tumour (SKOV-3) cells due to the presence of GGT. After 60 min of incubation with **17b**, an increasing fluorescence signal of a SKOV-3 tumour in mice was observed and, after 90 min, the tumour was clearly detectable.

Very recently, Yamaguchi and co-workers reported that the neutral, NIR-emissive D–A–A compound **18** (Scheme 4) can be injected in DMSO solution or in 18% DMSO in PBS with 1.6% BSA, respectively, to observe blood vessels in Japanese medaka larvae by confocal microscopy and in mice brains by two-photon excitation microscopy, respectively.[59]

4. Cationic triarylboranes

The attachment of cationic groups to a sterically-stabilised boron core can lead to water-soluble triarylboranes. The groups of Yang, in cooperation with S. Li and Y. Li, as well as of Marder, in cooperation with Blanchard-Desce, Meinel, Yamaguchi, Lambert, and Piantanida, showed that triarylborane (**19**, Scheme 5) and bis-triarylborane chromophores (**20–21**) equipped with cationic charges are all soluble in aqueous environments and cell permeable, as long as they are stable in water, and almost non-cytotoxic. The specifically designed

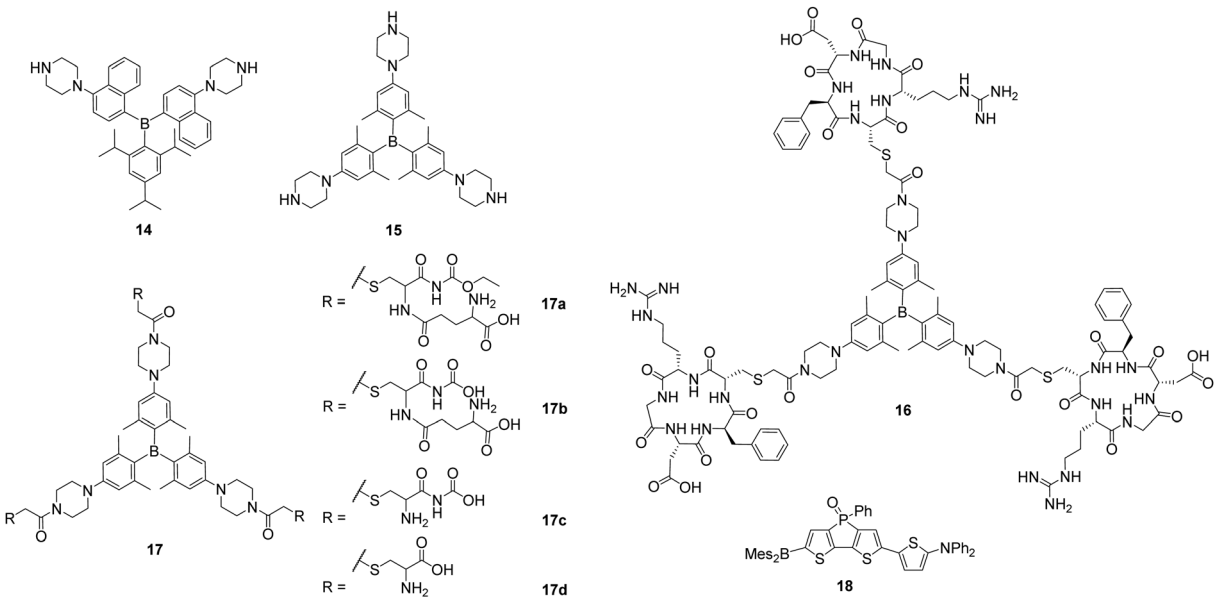

Scheme 4 Piperazine-substituted triarylboranes **14**, **15**, **16** and **17a–d** reported by Yang and co-workers.[22,27,28] Molecular structure of **18** reported by Baumgartner, Yamaguchi, and co-workers.[59]

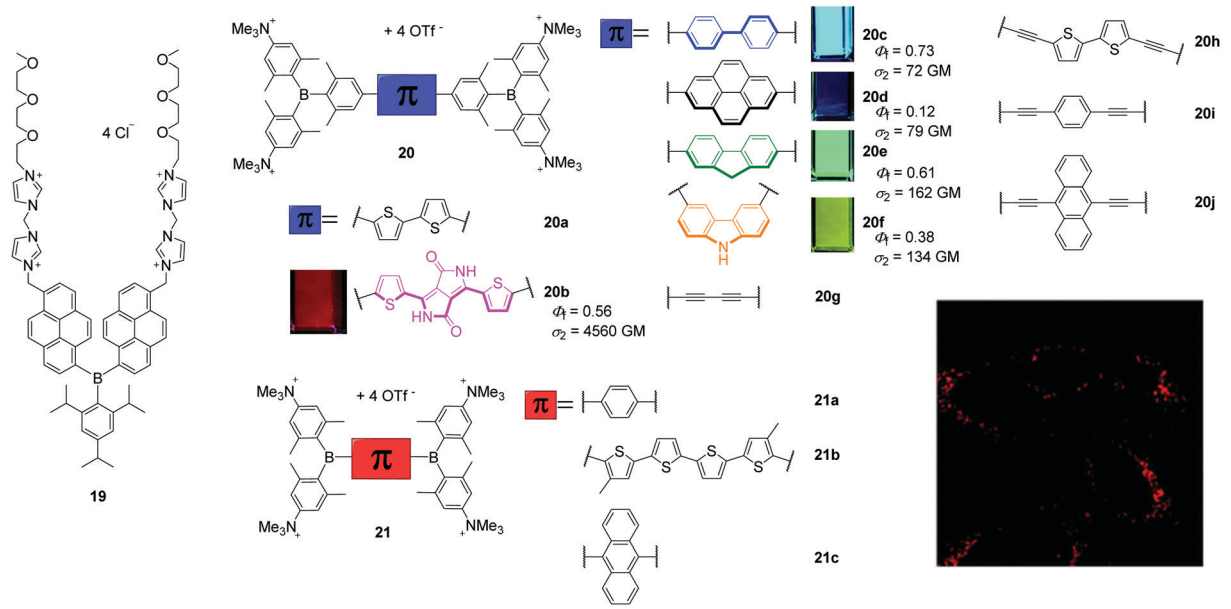

Scheme 5 Molecular structures of **19**[14,55] of Yang, S. Li, Y. Li and co-workers and **20a–j**,[17,26,30,60] **21a–c**[24] of Marder, Blanchard-Desce, Meinel, Yamaguchi, Lambert, Piantanida and co-workers. The small pictures show the emission of the compounds under UV irradiation in cuvettes when dissolved in acetonitrile. The fluorescence microscope image shows a high degree of localisation in the lysosomes of HeLa cells stained with **20b**. Coloured images are reproduced from ref. 26 with permission of The Royal Society of Chemistry.

triarylborane **19** selectively stains adenosine triphosphate (ATP) at the surface of mitochondria.[14,55] To the best of our knowledge, this was the first triarylborane applied in a cellular environment. Compound **19** bears two di(1*H*-imidazol-1-yl)methane dicationic groups, which account for its water-solubility, resulting in a detector that is selective for intracellular ATP, non-cytotoxic and stains cytoplasm and mitochondria. This was demonstrated by co-localisation experiments in NIH/3T3 cells, as was binding to the mitochondria due to ATP production by mitochondrial oxidative phosphorylation in eukaryotic cells, by pre-incubation experiments and FLIM measurements.

Marder and co-workers reported a series of tetracationic bis-triarylborane chromophores that selectively stain lysosomes (**20b–f**, **21a–c**, **23**, Scheme 5),[24–26] localise in protein environments in cells (**20a**),[17,31] the endoplasmic reticulum (**20g**)[30] or lysosomes and mitochondria simultaneously (**22**).[25] However, none of these compounds bears a motif that is structurally related to a biomolecule or known to direct the compound to a specific organelle inside the cell. Blanchard-Desce, Meinel, and Marder and co-workers reported the bithiophene bridged compound **20a** to be water-soluble, cell permeable, not cytotoxic to NIH/3T3, human embryonic kidney (HEK 293T) and HepG2-16 cells, and its absorption and emission spectra showed it to be more stable than the commercially available dye MitroTracker™ Red CMXRos (MTRC).[17] From one- and two-photon excited fluorescence spectroscopy of **20a** in fixed osteosarcoma tumour (POS-1) cells and extensive RNA-, DNA-, and protein-binding studies performed in cooperation with Piantanida and co-workers,[31] a hypsochromic shift of the emission maximum of **20a** in the cell compared to its emission spectrum in aqueous solutions was assigned to its binding to proteins in the cell. Thus, studying the interactions of the organoboranes with DNAs, RNAs and proteins in buffered solutions increased the information content of the cell imaging experiments. A series of related bis-triarylborane chromophores (**21a–c**) showed that significant steric hindrance is required to yield water-stability which is only provided by **21c** of this series and the previously reported compound **20a**.[24] Compound **21c** showed no cytotoxicity, was cell-permeable within 1 h and localises to a high degree at lysosomes as indicated by co-localisation experiments. Subsequently, compounds **20b–f** were synthesised to examine the effect of the bridging unit on the photophysical properties, cell viability, cell permeability and localisation in the cells (Scheme 5).[26] These five bis-triarylboranes were cell permeable, non-toxic to HeLa cells and their localisation at lysosomes was demonstrated by co-localisation experiments with different LysoTrackers™. Compound **20b** was shown to be taken up by the cell *via* the endocytosis pathway and has very good photostability, as 95% of the initial fluorescence intensity remained after irradiation for 12 min. Additionally, of the compounds in this series **20b** exhibits particularly red-shifted absorption and fluorescence spectra and an exceptionally high two-photon absorption cross-section (σ_2) of 4560 GM at 740 nm (Scheme 5). Another compound (**20g**) related to this series was reported to be non-cytotoxic to HeLa and HEK cells and the staining pattern obtained suggests binding to the endoplasmic reticulum, but co-localisation experiments have not yet been reported.[30] In addition, the interaction of **20g** with DNAs, RNAs, and proteins was investigated in buffered solutions *via* fluorimetry, surface-enhanced Raman scattering (SERS) and Raman spectroscopy revealing strong quenching of the emission and

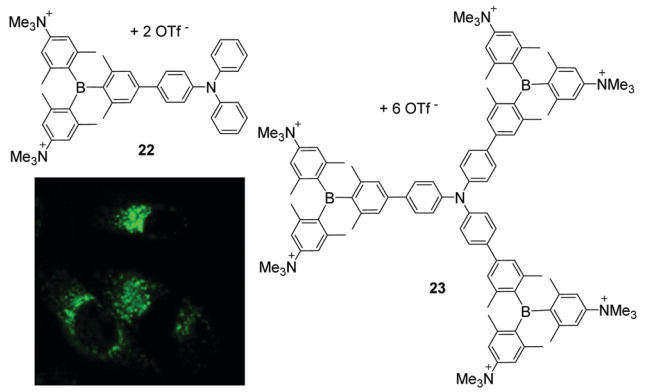

Scheme 6 Molecular structures of compound **22** and **23** by Marder, Yamaguchi, Lambert and co-workers.[25] The coloured picture displays the localisation of **23** in lysosomes of HeLa cells and is reproduced from ref. 25 with the permission of Wiley VCH.

enhancement of Raman signals upon binding. Very recently, this series was extended by three more alkyne-substituted bis-triarylboranes (**20h–20j**) which are also efficient dual fluorescence and Raman chromophores to detect DNA and RNA at very low concentrations in aqueous buffered solutions, strongly dependent on the bridging unit.[60]

Related dipolar and octopolar donor-π-acceptor compounds **22** and **23**, respectively, were shown to be soluble in water in the presence of 0.5% DMSO, non-cytotoxic to HeLa cells and cell permeable (Scheme 6).[25] Co-localisation experiments of **23** with LysoTracker™ Red (LTR) showed a high selectivity of this compound for accumulation in lysosomes. In contrast, **22** stains both lysosomes and mitochondria. The accumulation of both compounds can be monitored by two-photon excited fluorescence (TPEF) microscopy which provides deeper tissue penetration *via* NIR excitation in the 'biologically transparent window' and increases the 3D resolution of the images. Due to its higher two-photon brightness, lower toxicity, and higher selectivity for lysosomes, **23** is found to be a better candidate for bioimaging applications than **22**.

5. Discussion

A summary of the results obtained for staining of cell organelles with triarylboranes shows significant differences in the methods applied and the results obtained. For example, concentrations which cause cytotoxic effects vary drastically, even for very similar compounds (Table 1). Compounds **20d** and **20e** show no cytotoxic effects to HeLa cells up to concentrations of 5 μM whereas **20b** and **c** and **20f** are non-cytotoxic up to concentrations of 10 μM and **20g** was reported to be not cytotoxic up to concentrations of 100 μM. Surprisingly, the only difference between those molecules is the π-bridge connecting the two triarylborane moieties. Therefore, it might be concluded that, in the case of bis-triarylborane chromophores (**20**), the toxicity mainly results from various bridging units which was also shown to influence the mode of binding between these compounds and DNA, RNA or proteins in buffered solutions.[30,31,60]

In addition, the concentrations employed and incubation times are very different for the triarylboranes and commercially available dyes (Table 1). For example, staining of NIH/3T3 cells with **13b** + **2Cu**$^{2+}$ was reported after 5 min at concentrations of 10 μM whereas the commercial dye MTDF was used at a concentration of 0.1 μM with an incubation time of 30 min.[18] Thus, for the commercial dye, longer incubation times are required while the concentration used is lowered by 99%. Similarly, NIH/3T3 cells were incubated with **13b** + **2Zn**$^{2+}$ at 10 μM concentrations for 30 min while the concentrations used for the commercial dyes were as low as 5 μM for DiD and 75 nM for LTR DND-99.[29] Commercial dyes are used at lower concentrations but take longer to enter cells.

In some cases, the data for the same compound varies drastically, as described for **13b** (Table 1). On one hand, this compound was reported to stain NIH/3T3 cells at concentrations of 10 μM within 35 min,[21] but was also reported to stain the same cell line within 10 min using only 2 μM concentrations.[32]

Cytotoxicity tests for some of the compounds which have been applied to several cell lines, such as **13b**, **14**, **15**, and **17b**, and Pearson values (R_r, a measure of the degree of overlap of the images) for co-localisation studies with **13b**, **13b** + **2Zn**$^{2+}$, **14**, **15**, **16**, and **19a** have not been reported. Without cytotoxicity studies, it is not known whether the concentrations used for imaging experiments effect the viability of the cell line or, for compounds used in *in vivo* experiments such as **17b**, maybe even the animal. Interestingly, for **13b** + **2Zn**$^{2+}$, R_r values are given for some co-localisation experiments but not others (Table 1).[29] Without these correlation values, the degree of localisation in specific cell organelles is not known.

Given the observed differences in cytotoxicity, concentrations and incubation times, it would be useful for comparisons for there to be a standardised procedure for testing such new compounds. Standards exist for the characterisation of new compounds as their structure and purity are analysed by NMR and IR spectroscopy, mass spectrometry, X-ray diffraction, and elemental analysis with standard reporting protocols. In the field of organic photovoltaic and OLEDs, standardised methods exist for data collection and analysis to determine whether the respective absorbing or emitting layer improved the performance of the resulting device. Such standardisation is currently missing for chemists who want to examine the biological applicability of their triarylborane chromophores. Standardised protocols could include the use of at least one standard cell line by all research groups, together with uniform incubation times and concentrations. This would allow better comparison of the results obtained for different compounds by various groups. In addition, examination of the cytotoxicity of the chromophores to the standardised cell line prior to any *in vivo* experiments is highly recommended.

Table 1 Summary of cell experiments done with all triarylboranes mentioned in this review. c_{nc} = no cytotoxicity up to this concentration; c_{incub} = concentration of triarylboron compound used for incubation; t_{incub} = incubation time for triarylboron compound; c^{cd}_{incub} = concentration of commercial dye used for incubation; t^{cd}_{incub} = incubation time for commercial dye; N.R. = no data reported. – = not investigated. MTDF = Mito Tracker™ Deep Red FM; LTR = Lyso Tracker™ Red; MTRC = Mitro Tracker™ Red CMXRos; LTG = Lyso Tracker™ Green

Section	Compound	Cell line	c_{nc}	c_{incub}	t_{incub}	Dye for co-localisation	c^{cd}_{incub}	t^{cd}_{incub}	R_r
2	**7**[16]	NIH/3T3	0.4[a] μg mL^{-1}	—	—	—	—	—	—
	8[15]	NIH/3T3	1.0 μM	0.40 μM	30 min	—	—	—	—
	9[19]	NIH/3T3	0.4[a] μg mL^{-1}	N.R.	30 min	—	—	—	—
	NG-10[20]	NIH/3T3	0.4[a] μg mL^{-1}	10 μM	30 min	—	—	—	—
3	**11a**[23]	HeLa	15 μM	10 μM	30 min	—	—	—	—
	12a[23]	HeLa	15 μM	10 μM	30 min	—	—	—	—
	13a[21]	NIH/3T3	—	N.R.	1 h	—	—	—	—
	13b	NIH/3T3[21]	—	10 μM	35 min	SYTO™ RNAselect™	5 μM	35 min	N.R.
		NIH/3T3[21]	—	N.R.	5 min	—	—	—	—
		NIH/3T3[32]	Low toxicity[b]	2 μM	10 min	MTDF	0.1 μM	30 min	N.R.
		MCF-7[32]	Low toxicity[b]	2 μM	10 min	MTDF	0.1 μM	30 min	N.R.
		HepG2[32]	Low toxicity[b]	2 μM	10 min	MTDF	0.1 μM	30 min	N.R.
	13b + 2Cu^{2+}[18]	NIH/3T3	40 μM	10 μM	5 min	MTDF	0.1 μM	30 min	0.87
	13a + 3Zn^{2+}[29]	NIH/3T3	50 μM	N.R.	1 h	—	—	—	—
		HeLa	50 μM	—	—	—	—	—	—
		HepG2	50 μM	—	—	—	—	—	—
	13b + 2Zn^{2+}[29]	NIH/3T3	50 μM	10 μM	30 min	SYTO™ RNAselect™	0.5 μM	20 min	N.R.
						DiD	5 μM	30 min	N.R.
						LTR DND-99	75 nM	30 min	0.77
						MTDF	0.5 μM	45 min	0.85
						ER-tracker™ Red	1 μM	30 min	0.91
		HeLa	50 μM	N.R.	N.R.	—	—	—	—
		HepG2	50 μM	N.R.	N.R.	—	—	—	—
	14[22]	NIH/3T3	—	10 μM	30 min	SYTO™ RNAselect™	5 μM	30 min	N.R.
	15	NIH/3T3[22]	—	10 μM	30 min	SYTO™ RNAselect™	5 μM	30 min	N.R.
		NIH/3T3[27]	—	1 μM	15 min	—	—	—	—
		HUVEC-1[27]	—	1 μM	15 min	—	—	—	—
		U87MG[27]	—	1 μM	15 min	—	—	—	—
		NIH/3T3[28]	—	? μM[c]	5 min	—	—	—	—
	16[27]	NIH/3T3	5 μM	1 μM	15 min	—	—	—	—
		HUVEC-1	5 μM	1 μM	15 min	—	—	—	—
		U87MG	5 μM	1 μM	15 min	DiD red	5 μM	20 min	N.R.
	17b[28]	NIH/3T3	—	10 μM	1 h	—	—	—	—
		HUVEC	—	10 μM	1 h	—	—	—	—
		SKOV-3	—	10 μM	1 h	—	—	—	—
	17c[28]	NIH/3T3	—	? μM[c]	30 min	—	—	—	—
4	**19**[14,55]	NIH/3T3	4 μM	1 μM	30 min	MTDF	0.1 μM	30 min	0.86
	20a[17]	NIH/3T3	10 μM	10 μM	45 min	MTRC	0.125 μM	45 min	N.R.
		HEK293T	10 μM	—	—	—	—	—	—
	20a[17]	HepG2-16	10 μM	—	—	—	—	—	—
		POS-1	—	0.3 μM	8 h	—	—	—	—
	20b[26]	HeLa	10 μM	0.5 μM	2 h	LTG	0.1 μM	20 min	0.81
	20c[26]	HeLa	10 μM	0.5 μM	2 h	LTR	0.1 μM	20 min	0.80
	20d[26]	HeLa	5 μM	0.5 μM	2 h	LTR	0.1 μM	20 min	0.73
	20e[26]	HeLa	5 μM	0.5 μM	2 h	LTR	0.1 μM	20 min	0.75
	20f[26]	HeLa	10 μM	0.5 μM	2 h	LTR	0.1 μM	20 min	0.83
	20g[30]	HeLa	100 μM	1 μM	2 h	—	—	—	—
		HEK	100 μM	—	—	—	—	—	—
	21c[24]	HeLa	5 μM	5 μM	1 h	LTR	0.1 μM	20 min	0.86
	22[25]	HeLa	1 μM	0.5 μM	2 h	LTR	0.1 μM	20 min	0.48
						MTDR	0.05 μM	20 min	0.42
	23[25]	HeLa	1 μM	0.5 μM	2 h	LTR	0.1 μM	20 min	0.81

[a] Concentration used for cytotoxicity was reported in this unit by Hu, S. Li, Y. Li, Zhu, Zhang, and Shen, Yang and co-workers.[16,19,20] [b] No specific values were given in the text, and the supporting information was not accessible.[32] [c] Exact numbers were reported in the supporting information which was not accessible online.[28]

6. Conclusions

Triarylborane chromophores can respond to various changes in the cellular environment, *e.g.*, temperature, pH or to small molecules or biopolymers such as DNA, RNA, and proteins. They are often cell permeable and non-cytotoxic to various cell lines such as NIH/3T3, HEK, and HeLa cells, can localise in a variety of cell organelles, and can bind selectively to various DNAs, RNAs, and/or proteins. In addition, most of the compounds reported show one- and two-photon excited fluorescence and are more photostable than some commercial dyes, *e.g.*, MitoTracker™ or SYTO™ RNAselect™, and some can be used as dual fluorescence and Raman/SERS chromophores. Careful design of the compounds and collaboration among

synthetic chemists, experts in pharmaceutical chemistry, biochemistry, and bioimaging are important to move this field forward. Development of standardised protocols will also be helpful.

Author contributions

This review was drafted by SMB and revised by both authors.

Conflicts of interest

The authors declare no conflict of interest.

Acknowledgements

We thank the Deutsche Forschungsgemeinschaft (DFG; GRK 2112) and the Julius-Maximilians-Universität Würzburg for support.

References

1 L. Ji, S. Griesbeck and T. B. Marder, *Chem. Sci.*, 2017, **8**, 846–863.
2 C. D. Entwistle and T. B. Marder, *Angew. Chem., Int. Ed.*, 2002, **41**, 2927–2931.
3 C. D. Entwistle and T. B. Marder, *Chem. Mater.*, 2004, **16**, 4574–4585.
4 H. Zhao, L. A. Leamer and F. P. Gabbaï, *Dalton Trans.*, 2013, **42**, 8164–8178.
5 K. C. Song, K. M. Lee, N. V. Nghia, W. Y. Sung, Y. Do and M. H. Lee, *Organometallics*, 2013, **32**, 817–823.
6 H. R. Bhat, P. S. S. Gupta, S. Biswal and M. K. Rana, *ACS Omega*, 2019, **4**, 4505–4518.
7 V. Prakash Reddy, E. Sinn and N. Hosmane, *J. Organomet. Chem.*, 2015, **798**, 5–12.
8 P. A. Gale and C. Caltagirone, *Coord. Chem. Rev.*, 2018, **354**, 2–27.
9 G. Turkoglu, M. E. Cinar and T. Ozturk, *Molecules*, 2017, **22**, 1522.
10 B. M. Squeo and M. Pasini, *Supramol. Chem.*, 2020, **32**, 56–70.
11 T. M. Grant, D. S. Josey, K. L. Sampson, T. Mudigonda, T. P. Bender and B. H. Lessard, *Chem. Rec.*, 2019, **19**, 1093–1112.
12 Z. M. Hudson and S. Wang, *Dalton Trans.*, 2011, **40**, 7805–7816.
13 Y. Yu, C. Dong, A. F. Alahmadi, B. Meng, J. Liu, F. Jäkle and L. Wang, *J. Mater. Chem. C*, 2019, **7**, 7427–7432.
14 X. Li, X. Guo, L. Cao, Z. Xun, S. Wang, S. Li, Y. Li and G. Yang, *Angew. Chem., Int. Ed.*, 2014, **53**, 7809–7813.
15 X. Guo, X. Zhang, S. Wang, S. Li, R. Hu, Y. Li and G. Yang, *Anal. Chim. Acta*, 2015, **869**, 81–88.
16 J. Liu, X. Guo, R. Hu, J. Xu, S. Wang, S. Li, Y. Li and G. Yang, *Anal. Chem.*, 2015, **87**, 3694–3698.
17 S. Griesbeck, Z. Zhang, M. Gutmann, T. Lühmann, R. M. Edkins, G. Clermont, A. N. Lazar, M. Haehnel, K. Edkins, A. Eichhorn, M. Blanchard-Desce, L. Meinel and T. B. Marder, *Chem. – Eur. J.*, 2016, **22**, 14701–14706.
18 J. Liu, X. Guo, R. Hu, X. Liu, S. Wang, S. Li, Y. Li and G. Yang, *Anal. Chem.*, 2016, **88**, 1052–1057.
19 J. Liu, C. Zhang, J. Dong, J. Zhu, C. Shen, G. Yang and X. Zhang, *RSC Adv.*, 2017, **7**, 14511–14515.
20 J. Liu, C. Zhang, J. Dong, J. Zhu, C. Shen, G. Yang and X. Zhang, *New J. Chem.*, 2017, **41**, 4733–4737.
21 J. Liu, S. Zhang, C. Zhang, J. Dong, C. Shen, J. Zhu, H. Xu, M. Fu, G. Yang and X. Zhang, *Chem. Commun.*, 2017, **53**, 11476–11479.
22 J. Liu, S. Li, S. Zhang, C. Shen, J. Zhu, G. Yang and X. Zhang, *Sens. Actuators, B*, 2018, **261**, 531–536.
23 S. Pagidi, N. K. Kalluvettukuzhy and P. Thilagar, *Langmuir*, 2018, **34**, 8170–8177.
24 S. Griesbeck, M. Ferger, C. Czernetzi, C. Wang, R. Bertermann, A. Friedrich, M. Haehnel, D. Sieh, M. Taki, S. Yamaguchi and T. B. Marder, *Chem. – Eur. J.*, 2019, **25**, 7679–7688.
25 S. Griesbeck, E. Michail, F. Rauch, H. Ogasawara, C. Wang, Y. Sato, R. M. Edkins, Z. Zhang, M. Taki, C. Lambert, S. Yamaguchi and T. B. Marder, *Chem. – Eur. J.*, 2019, **25**, 13164–13175.
26 S. Griesbeck, E. Michail, C. Wang, H. Ogasawara, S. Lorenzen, L. Gerstner, T. Zang, J. Nitsch, Y. Sato, R. Bertermann, M. Taki, C. Lambert, S. Yamaguchi and T. B. Marder, *Chem. Sci.*, 2019, **10**, 5405–5422.
27 J. Liu, K. Cheng, C. Yang, J. Zhu, C. Shen, X. Zhang, X. Liu and G. Yang, *Anal. Chem.*, 2019, **91**, 6340–6344.
28 J. Liu, S. Zhang, B. Zhao, C. Shen, X. Zhang and G. Yang, *Biosens. Bioelectron.*, 2019, **142**, 111497.
29 J. Liu, S. Zhang, J. Zhu, X. Liu, G. Yang and X. Zhang, *Anal. Bioanal. Chem.*, 2019, **411**, 5223–5231.
30 H. Amini, Z. Ban, M. Ferger, S. Lorenzen, F. Rauch, A. Friedrich, I. Crnolatac, A. Kendel, S. Miljanic, I. Piantanida and T. B. Marder, *Chem. – Eur. J.*, 2020, **26**, 6017–6028.
31 Z. Ban, S. Griesbeck, S. Tomic, J. Nitsch, T. B. Marder and I. Piantanida, *Chem. – Eur. J.*, 2020, **26**, 2195–2203.
32 J. Dong, C. H. Zhang, B. Zhao, X. M. Zhang, Z. W. Leng and J. Liu, *Dyes Pigm.*, 2020, **174**, 108077.
33 B. R. Shaw, M. I. Dobrikov, X. Wang, J. Wang, K. He, J.-L. Lin, P. Li, V. Rait, Z. A. Sergueeva and D. S. Sergueev, *Ann. N. Y. Acad. Sci.*, 2003, **1002**, 12–29.
34 B. S. Burnham, *Curr. Med. Chem.*, 2005, **12**, 1995–2010.
35 A. Loudet and K. Burgess, *Chem. Rev.*, 2007, **107**, 4891–4932.
36 C. R. Wade, A. E. J. Broomsgrove, S. Aldridge and F. P. Gabbaï, *Chem. Rev.*, 2010, **110**, 3958–3984.
37 Z. Liu, Z. Jiang, M. Yan and X. Wang, *Front. Chem.*, 2019, **7**, 712.
38 K. Chansaenpak, B. Vabre and F. P. Gabbaï, *Chem. Soc. Rev.*, 2016, **45**, 954–971.
39 N. Boens, V. Leen and W. Dehaen, *Chem. Soc. Rev.*, 2012, **41**, 1130–1172.

40 Y. S. Marfin, A. V. Solomonov, A. S. Timin and E. V. Rumyantsev, *Curr. Med. Chem.*, 2017, **24**, 2745–2772.
41 C. S. Kue, S. Y. Ng, S. H. Voon, A. Kamkaew, L. Y. Chung, L. V. Kiew and H. B. Lee, *Photochem. Photobiol. Sci.*, 2018, **17**, 1691–1708.
42 C. A. Perks, A. J. Mill, G. Constantine, K. G. Harrison and J. A. B. Gibson, *Br. J. Radiol.*, 1988, **61**, 1115–1126.
43 K. Hu, Z. Yang, L. Zhang, L. Xie, L. Wang, H. Xu, L. Josephson, S. H. Liang and M.-R. Zhang, *Coord. Chem. Rev.*, 2020, **405**, 213139.
44 R. F. Barth and J. C. Grecula, *Appl. Radiat. Isot.*, 2020, **160**, 109029.
45 D. S. Novopashina, M. A. Vorobyeva and A. Venyaminova, *Front. Chem.*, 2021, **9**, 619052.
46 A. Paramore and S. Frantz, *Nat. Rev. Drug Discovery*, 2003, **2**, 611–612.
47 S. Gronowitz, Y. Zhang and A.-B. Hörnfeldt, *Acta Chem. Scand.*, 1992, **46**, 654–660.
48 K. E. Broaders, S. Grandhe and J. M. Frechet, *J. Am. Chem. Soc.*, 2011, **133**, 756–758.
49 C. Achilli, A. Ciana, M. Fagnoni, C. Balduini and G. Minetti, *Cent. Eur. J. Chem.*, 2013, **11**, 137–139.
50 K. C. Yan, A. C. Sedgwick, Y. Zang, G. R. Chen, X. P. He, J. Li, J. Yoon and T. D. James, *Small Methods*, 2019, **3**, 1900013.
51 E. A. Veal, A. M. Day and B. A. Morgan, *Mol. Cell*, 2007, **26**, 1–14.
52 C.-W. Chiu, Y. Kim and F. P. Gabbaï, *J. Am. Chem. Soc.*, 2009, **131**, 60–61.
53 Y. Kim and F. P. Gabbaï, *J. Am. Chem. Soc.*, 2009, **131**, 3363–3369.
54 T. Agou, M. Sekine, J. Kobayashi and T. Kawashima, *Chem. – Eur. J.*, 2009, **15**, 5056–5062.
55 X. Li, X. Guo, L. Cao, Z. Xun, S. Wang, S. Li, Y. Li and G. Yang, *Angew. Chem.*, 2014, **126**, 7943–7947.
56 S. Mukherjee and P. Thilagar, *J. Mater. Chem. C*, 2016, **4**, 2647–2662.
57 Y. Ma, J. Yin, G. Li, W. Gao and W. Lin, *Coord. Chem. Rev.*, 2020, **406**, 213144.
58 L. Feng and Y. Zhao, *View*, 2020, **1**, e15.
59 Y. Sugihara, N. Inai, M. Taki, T. Baumgartner, R. Kawakami, T. Saitou, T. Imamura, T. Yanai and S. Yamaguchi, *Chem. Sci.*, 2021, **12**, 6333–6341.
60 M. Ferger, Z. Ban, I. Krosl, S. Tomic, L. Dietrich, S. Lorenzen, F. Rauch, D. Sieh, A. Friedrich, S. Griesbeck, A. Kendel, S. Miljanic, I. Piantanida and T. B. Marder, *Chem. – Eur. J.*, 2021, **27**, 5142–5159.

